Bioinformatics, 36(1), 2020, 154–159
doi: 10.1093/bioinformatics/btz527
Advance Access Publication Date: 28 June 2019
Original Paper

Structural bioinformatics

A helical lock and key model of polyproline II conformation with SH3

Tomer Meirson [1,2,*], David Bomze[3], Liron Kahlon[4], Hava Gil-Henn[2] and Abraham O. Samson[1]

[1]Drug Discovery Laboratory, The Azrieli Faculty of Medicine, [2]Laboratory of Cell Migration and Invasion, The Azrieli Faculty of Medicine, Bar-Ilan University, Safed 1589, Israel, [3]Sackler Faculty of Medicine, Tel Aviv University, Tel Aviv 39040, Israel and [4]The Azrieli Faculty of Medicine, Bar-Ilan University, Safed 1589, Israel

*To whom correspondence should be addressed.
Associate Editor: Arne Elofsson

Received on March 7, 2019; revised on June 9, 2019; editorial decision on June 19, 2019; accepted on June 24, 2019

Abstract

Motivation: More than half of the human proteome contains the proline-rich motif, PxxP. This motif has a high propensity for adopting a left-handed polyproline II (PPII) helix and can potentially bind SH3 domains. SH3 domains are generally grouped into two classes, based on whether the PPII binds in a positive (N-to-C terminal) or negative (C-to-N terminal) orientation. Since the discovery of this structural motif, over six decades ago, a systematic understanding of its binding remains poor and the consensus amino acid sequence that binds SH3 domains is still ill defined.

Results: Here, we show that the PPII interaction with SH3 domains is governed by the helix backbone and its prolines, and their rotation angle around the PPII helical axis. Based on a geometric analysis of 131 experimentally solved SH3 domains in complex with PPIIs, we observed a rotary translation along the helical screw axis, and separated them by 120° into three categories we name α (0–120°), β (120–240°) and γ (240–360°). Furthermore, we found that PPII helices are distinguished by a shifting PxxP motif preceded by positively charged residues which act as a structural reading frame and dictates the organization of SH3 domains; however, there is no one single consensus motif for all classified PPIIs. Our results demonstrate a remarkable apparatus of a lock with a rotating and translating key with no known equivalent machinery in molecular biology. We anticipate our model to be a starting point for deciphering the PPII code, which can unlock an exponential growth in our understanding of the relationship between protein structure and function.

Availability and implementation: We have implemented the proposed methods in the R software environment and in an R package freely available at https://github.com/Grantlab/bio3d.

Contact: Tomermrsn@gmail.com

Supplementary information: Supplementary data are available at *Bioinformatics* online.

1 Introduction

Proline-rich motifs (PRM) are peptide segments, containing multiple proline residues, which recognize a variety of protein folds (Kuriyan and Cowburn, 1997; Pawson and Scott, 1997; Zarrinpar *et al.*, 2003). Deciphering the recognition of PRMs, which are included in 62% of the human proteome (Ravi Chandra, 2004), is of paramount importance for better understanding protein–protein interactions regulating many signal transduction pathways. One large and well characterized protein fold recognized by PRMs is the Src-homology 3 (SH3) domain family (Mayer and Eck, 1995). SH3 domains consist of ~60 amino acids and recognize PRMs through a collection of binding pockets and grooves. At one end, the SH3 domain contains a binding pocket, dubbed the specificity site, formed by the N-Src and RT loops (Fig. 1A) which mainly recognizes positively charged peptide residues, Arg/Lys, and directs the peptide backbone binding

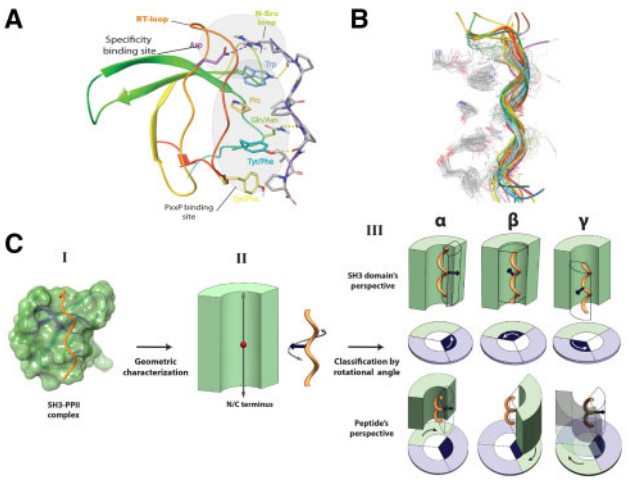

Fig. 1. SH3 domain interaction with PPII. (**A**) Representative crystal structure of SH3 domain in complex with a peptide ligand (PDB ID: 1QWF). Salt bridge interactions and H-bonds are shown in stippled lines. Note the negatively charged SH3 specificity site which binds a positively charged peptide residue. Note the PxxP-binding site which forms hydrophobic interactions and hydrogen bonds with the peptide backbone residues. (**B**) Superposition of SH3 domains in complex with their cognate ligands. The peptide and the conserved SH3 domain residues involved in the interaction are shown in sticks, and the peptide backbone is displayed. (**C**) Classification scheme: (**I**) Peptides in complex with SH3 domains were evaluated for adopting a PPII conformation. (**II**) The relative orientation between the SH3 and the center of the PPII was used to determine the angular rotation. (**III**) Based on the angle (black 3D arrow), the complexes were classified into three groups α, β and γ separated by 120°. From the SH3 domain's perspective the transition from class to class (left-to-right) is associated with an anti-clockwise rotation of the ligand and vice versa

orientation either from N- to C- (class I), or from C- to N-terminus (class II) (Feng *et al.*, 1994; Mayer, 2001). Adjacently, SH3 domains also contain a binding surface with two hydrophobic grooves, named the PxxP-binding site (Nguyen *et al.*, 2000). This binding surface is adapted for recognition of a left-handed polyproline II (PPII) helix with three residues per turn which is the third most common type of secondary structure in folded proteins (Adzhubei *et al.*, 2013). The recognition mechanism has been described both as discriminatory, and as promiscuous which has led to speculations on how and why this alleged contradiction is favored by evolution and why nature has targeted the PPII motif for binding domains (Agrawal and Kishan, 2002; Ball *et al.*, 2005; Li, 2005).

For many years, the consensus amino acid sequence of PPII recognizing SH3 domains has been vague (Li, 2005). While most ascertain a core sequence which includes PxxP, the consensus sequences have been written in various forms in the literature and it is unclear what distinguishes a typical from an atypical sequence (Kaneko *et al.*, 2008; Kay *et al.*, 2000; Tossavainen *et al.*, 2016). Furthermore, the consensus sequence is embroiled by the parallel and antiparallel dimerization of SH3 with PPII and their dual capacity to bind both positive (class I) and negative (class II) orientations, that matches the motifs +xxPxxP and xPxxPx+, respectively, where + denotes a positively charged residue, x any residue and P a proline residue (Kaneko *et al.*, 2008).

This dual classification scheme of PPII based solely on peptide orientation is insufficient for this large family of PRMs and fails to explain the high amount of non-consensus peptide sequences that readily bind SH3 domains (Ball *et al.*, 2005; Saksela and Permi, 2012). Several studies have tried to expand the classification scheme by surveying the specificity landscape of human SH3 domains using high throughput binding assays (Carducci *et al.*, 2012; Teyra *et al.*, 2017); however, some aspects of the binding mechanism were disregarded and the resulting canonical specificities disagree with solved structures in ~50% of the cases (Teyra *et al.*, 2017). In view of the current understanding of PPII, that is characterized by disjointed motifs and patterns, a more detailed, coherent and unified model is required.

2 Materials and methods

2.1 Data collection

To obtain all SH3 domain complexed with PPII helices, we queried the PDB database for 'SH3' in all species which resulted in 928 PDB files. Each SH3 domain was inspected manually and downloaded if it involved an interaction with a peptide. In total, we identified 131 PDB files with SH3–peptide complexes (Supplementary Table S1). Crystal structures with several chains and NMR structures with multiple conformations were split into separate complexes which resulted in a total of 615 SH3–peptide complexes. Peptides with <6 residues in the PxxP-binding groove or synthetic residues in this interface were excluded. Crystal structures with a resolution above 3 Å were also excluded. We used Bio3D package (Grant *et al.*, 2006) in the statistical programming language R (https://www.r-project.org/) to analyze the structures.

2.2 Binding frame assignment

The 6-residue reading frame representing the PxxP-binding interface was assigned based on the position of the peptide relative to the conserved residue next to the specificity site, which is usually Trp (Hu and Settleman, 1997). Since PPII peptides contain several important residues that can be situated in various ways and orientations, we used a uniform nomenclature that is based only on the PxxP-binding frame. The most N-terminal residue in this frame is assigned as position '1' and the remaining positions increment positively towards the C-terminal direction and negatively towards the N-terminal direction. This allows a comparable nomenclature that is independent of the peptide orientation.

2.3 Polyproline Type II assignment

Given the complexity and the milieu of sequences and conformations, assignment tools are limited and there is not a single acceptable approach to assign PPII to a peptide (Mansiaux *et al.*, 2011). Therefore, we used the torsional angle space of the identified complexes to define the averaged PPII. Thus, we calculated the root-mean-square dihedral deviations (RMSdD) of the peptide backbone torsional angles ϕ and ψ as a measure of the average deviation from the reference PPII. The RMSdD of ϕ and ψ angles is given by

$$\mathrm{RMSdD}_{\phi} = \sqrt{\frac{1}{N}\sum_{i=1}^{N}(\phi_i - \phi_r)^2} \quad (1)$$

$$\mathrm{RMSdD}_{\psi} = \sqrt{\frac{1}{N}\sum_{i=1}^{N}(\psi_i - \psi_r)^2} \quad (2)$$

where N is the total number of residues with calculated torsional angles ϕ_i and ψ_i, and ϕ_r and ψ_r are the reference angles of $\phi = -78°$, $\psi = 146°$ (Stapley and Creamer, 1999). The mean RMSdD that incorporates both torsional dihedral angles is then given by

$$\mathrm{RMSdD} = \frac{\mathrm{RMSdD}_{\phi} + \mathrm{RMSdD}_{\psi}}{2} \quad (3)$$

The histogram of RMSdD and the threshold of assignment is shown in Supplementary Fig. S1.

2.4 Sequence alignment

Sequence alignment was performed using Bio3D and MUSCLE (Edgar, 2004) according to the assigned class. For ensemble structures, the class was assigned based on the averaged structure. Logo sequences were drawn using ggseqlogo (Wagih, 2017).

3 Results

3.1 Classification scheme of the rotating helical PPII

To include only structures with PPII conformation, we developed a method to assign PPIIs based on their deviations from a reference PPII configuration (Supplementary Table S2 and materials). We used the assigned PPII–SH3 domain complexes to depict a variety of binding modes (Fig. 1B). We hypothesize that the peptides are characterized by a rotation coupled with translation (i.e. screw motion) along the helix axis, compared to a common reference point (Fig. 1B). Since every three residues complete a PPII turn (Kaneko *et al.*, 2008), we propose to divide the complexes into three classes α (0–120°), β (120–240°) and γ (240–360°) separated by 120° (Fig. 2C). Note that this classification does not interfere with positive/negative class nomenclature, and that α, β and γ can be positive or negative (i.e. α^-, γ^+) (Supplementary Table S3). Since two SH3 domains can bind to a single peptide simultaneously, a peptide can be classified both as α^- vis-à-vis one SH3 domain, and as γ^+ vis-à-vis another SH3 domain. For example, in the complex formed between one PPII and two SH3 domains (PDB: 2BZ8), our analysis showed that one SH3 domain binds a class α^- PPII, while the other SH3 binds a class γ^+ PPII (Fig. 2A and B). In this example, the two SH3 domains interact via their N-SRC loops. In another example (PDB: 2D1X), our analysis showed that one SH3 domain binds a class β^- PPII, while the other SH3 domain binds a class γ^+ PPII. In this example, the SH3 domains interact via their RT loops (Fig. 2A and B). In addition, the overlap of the two dimers (Fig. 2a, bottom) demonstrates how the domains encircle the peptide with a 3-fold pseudosymmetry, where each domain is separated by 120° (Fig. 2B). Remarkably, there is no example in the PDB of a dual class α/β peptide in complex with two SH3, only examples with β/γ or α/γ

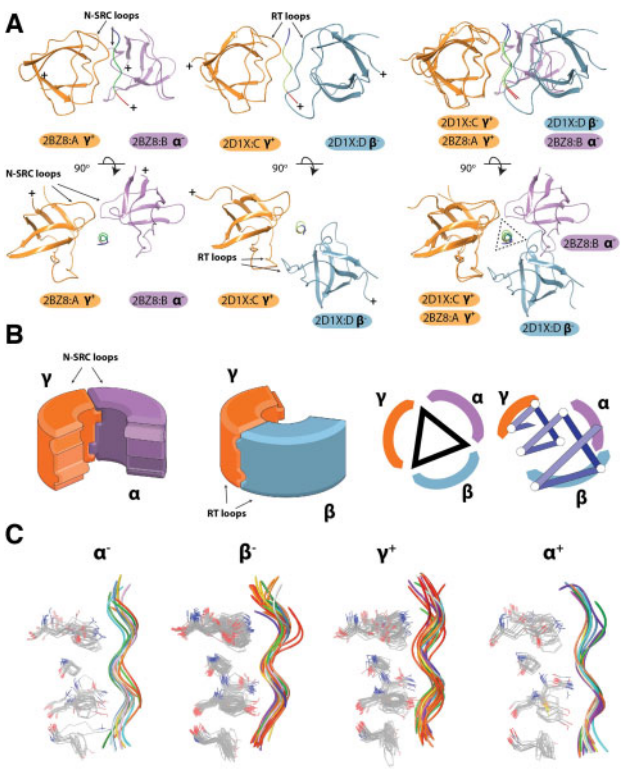

Fig. 2. Rotation-based classification of PPII/SH3 complexes. (**A**) The structures of a single peptide in complex with two SH3 domains. In 2BZ8, one SH3 domain is positively oriented towards the peptide facing its γ side, and one is negatively oriented facing its α side. In 2D1X, one SH3 domain is positively oriented towards the peptide facing its γ side, and one is negatively oriented facing its β side. Steric hindrance prevents SH3 domain from binding to all faces (α, β and γ) and encircling the peptide in a 3-fold pseudosymmetry. The N-terminus of the proteins is designated by a plus (+) sign. The three symmetrical interfaces are emphasized using a stippled triangle (bottom right). (**B**) The classifications of SH3–PPII complexes are illustrated for SH3 dimers (left) and for the peptide (right) as a 2D projection and in 3D view. (**C**) Shown are superimposed peptides categorized by class and orientation of all SH3–peptide complexes in the dataset. The conserved SH3 residues of the binding site are shown in stick representation

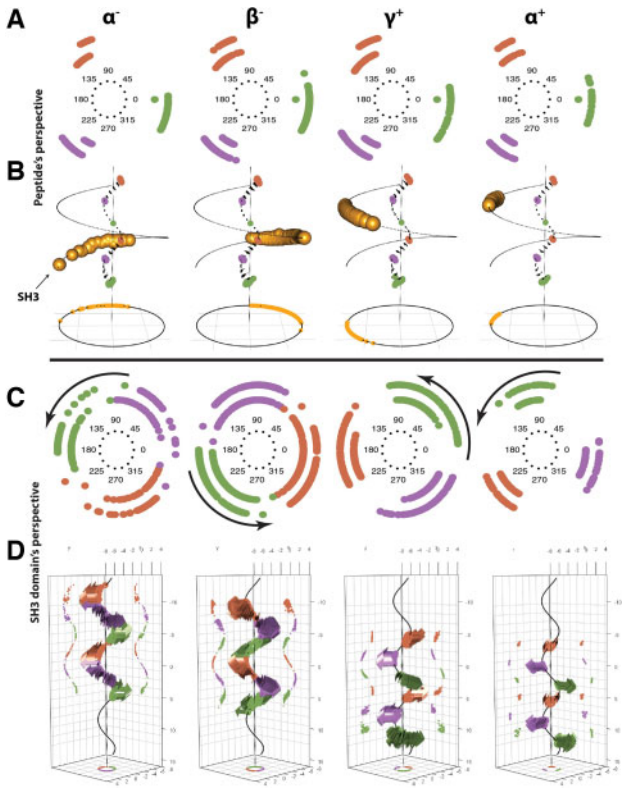

Fig. 3. Polyproline Type II sliding helix pattern. The residue angles of all PPIIs in the dataset are shown as a projection (**A**) and in 3D (**B**) from the peptide's perspective (the reference is set to the third PPII residue), demonstrating a similar distribution between classes. Red, purple and green dots represent the first, second and third residues of each PPII turn, respectively. The first and second turns are designated by the inner and outer circles, respectively. The angular position and projection (B) of the conserved SH3 proline (indicated by orange spheres) demonstrate a helical screw pattern. The residue angles of all PPIIs in the dataset are shown as a projection (**C**) and in 3D (**D**) from the target's perspective (the reference is set to the conserved proline in SH3 domain). These distributions depict an anti-clockwise rotation along a sliding helical path [shown in black arrows (C) and curves (D)]. These observations indicate that the interaction is characterized by a gradual shift in PPII position and is independent of conformational changes within the peptide. Perpendicular arrows and X, Y and Z projections are shown to aid in the spatial interpretation. Z axes are in radians. Each panel is stratified into four columns α^-, β^-, γ^+ and α^+

(Fig. 2). Figure 3A and B show that 3D conformation (and 2D projection) of the peptides is very similar between classes. However, the relative position of a peptide to SH3 domain depends on the class, and vary by 120° in α, β and γ (Fig. 3C and D). This interesting pattern indicates that the peptides are not distinguished by conformational changes within their structure but between their binding target. Each peptide (or class) is characterized by a gradual rotation and translation and is partitioned hierarchically, where α^+ and α^- are separated by a complete turn. The rotary distributions are continuous, except for a small region spanning between β^- and γ^+, suggesting an unfavored position at the interface between positive and negative orientations. The distribution can be described as a rotating corkscrew that is distinguished by the relative rise of the peptide. A similar pattern is observed from the peptides' perspective, where the SH3 domains encircle the ligand in an imaginary cylinder oriented along the helix axis (Fig. 3B).

3.2 The dynamic helical motion of PPII

NMR ensemble structures with multiple conformers provide valuable insight into the dynamic motion of proteins and their complexes. Such insight for the SH3 bound PPII (PDB: 1RLP) demonstrates a range of binding modes that follows a helical path (Supplementary Fig. S2A–C and Table S4) which agrees with a corkscrew motion. The rotation and translation of the helix are coupled with intermolecular interactions formed in the specificity zone of SH3, by the hydrogen bonds and basic amino acid residues which affect the position and the range of motion and even enable a transition between classes (Supplementary Fig. S2B). This observation also explains how peptides bind targets differently despite sharing an identical sequence. This idea is also supported by the peptides PDB 4Z88 chains M, P and S which differ only by the amount of arginine residues that form salt bridges, and cause a clockwise or counterclockwise rotation (Supplementary Fig. S3A and C). Furthermore, chain M which has only one additional arginine displays the same binding mode as chain O, indicating that the flanking regions control or stabilize the binding mode but are not obligatory as the peptide can bind equivalently regardless of the flanking residues (Supplementary Fig. S3B).

3.3 The rotating PxxP pattern

To analyze the consensus sequence, we aligned the sequences according to their class and designate the residues in contact with the PxxP-binding grooves as structural reading frames. In this context, the reading frame consists of two triplicate residues which serve as structural 'codons'. The terminological use of structural protein 'codons' is supported by the formation of a complete turn by each triplicate and the periodic repeats of three residues found in the majority of proline-rich target sequences (Ball *et al.*, 2005). The alignment demonstrates the known motifs for positive (xxPxxP) and negative (xPxxPx) orientations that are flanked mainly by positively charged residues at the start (N-terminus) or end (C-terminus) sites (Fig. 4A). Introducing a shift in the position to correct for structural positioning reveals a shifting pattern in the PxxP motif (Fig. 4A). Translating the shifting pattern of the positive and negative consensus sequences into a circular diagram demonstrates how α^- and α^+ differ by a complete turn (Fig. 4B). Despite the pattern in the PxxP motif, the alignment (Fig. 4A) indicates that there is no unique consensus sequence for each class.

3.4 Structural organization of the tripartite complex

Two SH3 domains may interact with one PPII through antiparallel dimerization and orient the SH3 conserved prolines of the PxxP-binding sites such that they face towards the PPII (Supplementary Fig. S4). In this configuration, up to three chains (one PPII peptide and two SH3 domains) form coiled-coils, reminiscent of leucine zippers. We name this structural motif, containing proline-rich coiled-coil, 'proline zipper'. Figure 4C lays all the observed mode of interactions between SH3 monomers and proline zippers. Figure 4D and E shows that the assigned class based on the calculated rotational angle of the peptide to each of the monomers, agrees with the distinct circular separation about the rotational axis by 120°, where α/γ dimers interact via the N-Src loops and β/γ via the RT loops. Remarkably, Fig. 4D and E demonstrate that some PPIIs encode also a longitudinal displacement over the helix axis arising from a shift of the reading frame. Notably, since peptides are placed within a rotational continuum, the classification into two groups

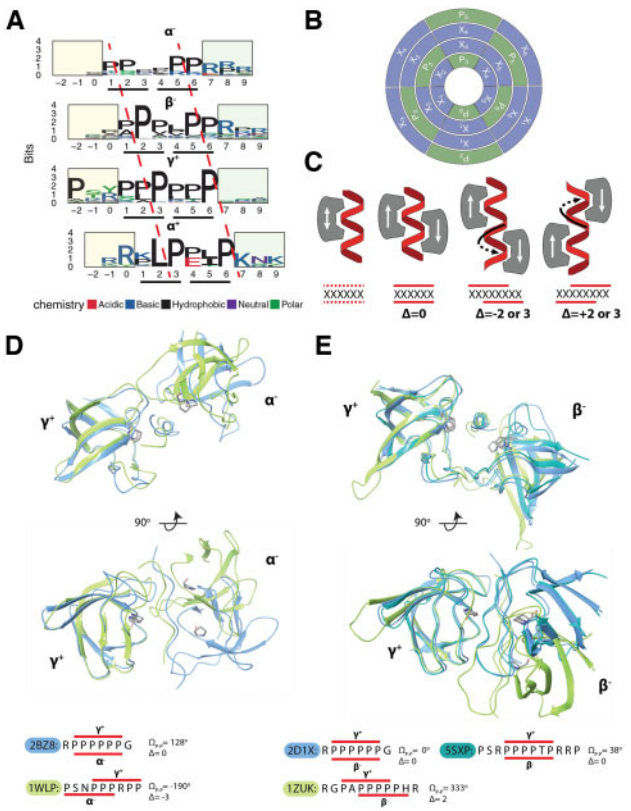

Fig. 4. SH3–PPII complexes are governed by structural reading frames. (**A**) PPII sequences aligned based on structural position relative to the SH3 binding site, grouped into four classes. Sequence logo of classes α^- and α^+ were adjusted to match the relative position of β^-, γ^+, respectively. The first (positions 1–3) and the second (positions 4–6) structural codons denote the reading frame and the flanking 'specificity site' binding residues are represented by start (left square) and end sites (right square). The dashed lines mark the shifting core PxxP motif. (**B**) Circular diagram showing the consensus sequences of positive (xPxxPx) and negative (xxPxxP) orientations. The consensus sequences of α^-, β^-, γ^+ and α^+ classes are represented by layers (outer to inner) in which α^- and α^+ were adjusted to match the relative position of β^-, γ^+, respectively. The diagram shows how α^- and α^+ are spaced by a complete circle. (**C**) Illustrations depicting the possible types of SH3–PPII interactions emphasizing the vertical displacement of the protein complex assembly. The SH3 monomers (left) or dimers bind PPII in either the positive or negative orientations designated by arrows. The shape and the helix represent the conserved SH3 proline and PPII, respectively. Solved SH3–PPII dimers are observed as α^-/γ^+ (**D**) or β^-/γ^+ (**E**). X denotes any residue and Δ is the residue interval between the reading frames marked by lines. Ω_{P-P} designates the angular separation between the SH3 dimers around the PPII helix. Conserved SH3 prolines are shown in sticks

(class I/II), three ($\alpha/\beta/\gamma$), or any discrete group, is artificial and subjective. Nonetheless, our proposed classification is expected to be useful especially for assigning the spatial organization of SH3 dimers, characterized by 3-fold pseudosymmetry as seen in Fig. 4D and E.

4 Discussion

Fischer's lock and key model proposes that biomolecular interactions are driven by shape complementarity (Koshland, 1995). Complementary binding partners with essentially random spatial arrangements require focused investigation into the specific interactions to reveal the unique aspects of the binding mechanism. Furthermore, in evolutionary terms, the development of binding partners relies on multiple changes and the complexity is further complicated for multi-domain assemblies.

Here, we discover that the interaction between SH3 domain and PPII is governed by a helical screw displacement that conforms to a lock and a helical key model (Fig. 5A and B). This unique mechanism explains how the PPII sequence not only encodes the binding mode but also the organization in multi-domain assemblies. Additionally, this conserved apparatus allows an efficient evolutionary way to completely change the selectivity profile and consequent function using a single substitution (Bergamaschi *et al.*, 2006; Hansson *et al.*, 1995; Leusen *et al.*, 1994), or to regulate the binding spatially and temporally by fine-tuning the interactions with the flanking regions.

The significance of PPII cannot be overestimated not only because of its wide presence in cellular signaling, but also due to the direct involvement in various diseases, including cancer (Adzhubei *et al.*, 2013; Bergamaschi *et al.*, 2006; Hansson *et al.*, 1995; Leusen *et al.*, 1994; Narwani *et al.*, 2017). This is exemplified especially by the most common genetic alteration (Bergamaschi *et al.*, 2006) within the most mutated gene in human cancer—TP53 (Hamelin *et al.*, 1994), where a single substitution of Arg72 with Pro72 in the PPII sequence induces a switch between an apoptotic state to G1 arrest and DNA repair (Khrunin *et al.*, 2010).

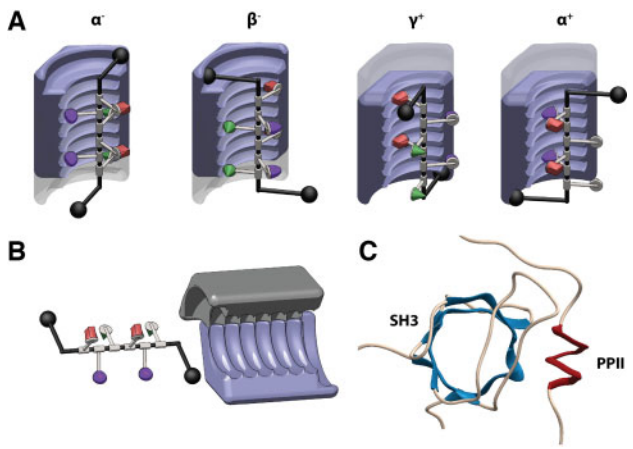

Fig. 5. Helical lock and key model. (**A**) Graphical representation of SH3 domain (the lock) and the helical peptide ligand (key) grouped in four hierarchical classes. Each interaction is characterized by a specific rotational angle along a helical path, where the negative (α^- and β^-) and positive (γ^+ and α^+) SH3 orientations, form a continues thread for the helical ligand. The cuboid, spherical and pyramid shapes represent the first, second and third residues of each turn, respectively, and black spheres represent the flanking residues. (**B**) A helical key that conforms to a combination of antiparallel SH3 domains results in a protein complex assembly. (**C**) Proposed graphical rendering of the secondary structure of PPII bound to SH3 domain emphasizing the triangular properties of the helix

This study is the first to report that PPIIs exhibit a helical motion based on the analysis of ensemble structures. The inherent dynamic property of the peptide is influenced and restricted by specific formations in the target SH3 domain. This implies that an altered construction may allow a full rotational motion, acting as a molecular gear, such as a worm gear, to produce physical propagation. This hypothesis is corroborated by the presence of the motif in proteins that direct displacement and facilitate motion, including the direct involvement of motor proteins in flagellar motility (Braun *et al.*, 1999; Obuchowski and Jacobs-Wagner, 2008), titin in sarcomere contraction (Ma *et al.*, 2001), dynamin in endocytosis (Luo *et al.*, 2016), PRRT2 in neurotransmitter exocytosis (Coleman *et al.*, 2018) and profilin in actin polymerization and invadopodia dynamics (Valenzuela-Iglesias *et al.*, 2015).

Although PPII is the common name used to describe the motif, the term has been widely criticized (Adzhubei *et al.*, 2013; Hollingsworth *et al.*, 2009; Mansiaux *et al.*, 2011; Martin *et al.*, 2014) for its misleading association with only prolines while many such structures contain few or none (Mansiaux *et al.*, 2011; Narwani *et al.*, 2017). Moreover, this term may not consistently recapitulate the extensive conformational space exhibited by the motif (Adzhubei *et al.*, 2013). Hence, we propose the name 'κ-helix' which abides the tradition of Latin letters to secondary structures and because it is composed of three lines that form three rotating triangles. In addition, 'Kappa', begins with a positively charged residue (K), enriched with prolines (or polyproline, PP) and any residue, A with a slight preference for aliphatic residues). Furthermore, AppA symbolizes the triple residues needed to complete a turn.

Due to the increasing realization of the importance and prevalence among secondary structures (Adzhubei *et al.*, 2013; Mansiaux *et al.*, 2011) and due to the triangular geometrical properties, we suggest a novel graphical presentation (Fig. 5C) to aid in interpreting the structure that is currently blind to the observer. The proposition to include PPII into the mainstream, such as α-helices and β-sheets, was advocated as early as 1993 (Adzhubei and Sternberg, 1993). The proposed model allows to characterize the interaction between the PPII helix and its target using a unique angle; however, it is important to highlight that the accuracy relies on the quality of the structures. Future investigation should explore the molecular determinants underlying specific rotational angles for each SH3 domain and the relationship between the binding energies and rotational angles. Also the question of whether the helical lock and key model of PPII conformations applies only to SH3 domains or is a general phenomenon found in other PRM families, such as WW, GYF and EVH1 domains (Ball *et al.*, 2005), should be examined.

For decades, scientists have been intrigued how a short, simple and very similar sequence characterized by promiscuity can regulate specific functions. Based on available experimental data, we find a clear pattern of a rotating helical motif, and a consensus sequence that governs the structural relationship between PPII and SH3 domains. Our results illustrate a model that lays the foundation for the recognition of proteins by PPII and constitute a significant contribution towards unveiling the determinants of the master key which will enable to unlock a plethora of biological locks.

Funding

This work was supported by the Leir Foundation and the Ginzburg Foundation (to Abraham O. Samson), and by the Israel Cancer Association and Estee Lauder Companies (grant No. 20180089), the Israel Cancer Research Foundation (grant No. 17-902-AG) and the Israel Science

Foundation (grant No. 1462/17) (to Hava Gil-Henn). Tomer Meirson was supported by the Foulkes Foundation fellowship for MD/PhD students.

Conflict of Interest: none declared.

References

Adzhubei,A.A. and Sternberg,M.J. (1993) Left-handed polyproline II helices commonly occur in globular proteins. *J. Mol. Biol.*, **229**, 472–493.

Adzhubei,A.A. *et al.* (2013) Polyproline-II helix in proteins: structure and function. *J. Mol. Biol.*, **425**, 2100–2132.

Agrawal,V. and Kishan,K. (2002) Promiscuous binding nature of SH3 domains to their target proteins. *Protein Peptide Lett.*, **9**, 185–193.

Ball,L.J. *et al.* (2005) Recognition of proline-rich motifs by protein–protein-interaction domains. *Angew. Chem. Int. Ed.*, **44**, 2852–2869.

Bergamaschi,D. *et al.* (2006) iASPP preferentially binds p53 proline-rich region and modulates apoptotic function of codon 72–polymorphic p53. *Nat. Genet.*, **38**, 1133.

Braun,T.F. *et al.* (1999) Function of proline residues of MotA in torque generation by the flagellar motor of *Escherichia coli*. *J. Bacteriol.*, **181**, 3542–3551.

Carducci,M. *et al.* (2012) The protein interaction network mediated by human SH3 domains. *Biotechnol Adv.*, **30**, 4–15.

Coleman,J. *et al.* (2018) PRRT2 regulates synaptic fusion by directly modulating SNARE complex assembly. *Cell Rep.*, **22**, 820.

Edgar,R.C. (2004) MUSCLE: multiple sequence alignment with high accuracy and high throughput. *Nucleic Acids Res.*, **32**, 1792–1797.

Feng,S. *et al.* (1994) Two binding orientations for peptides to the Src SH3 domain: development of a general model for SH3-ligand interactions. *Science*, **266**, 1241–1247.

Grant,B.J. *et al.* (2006) Bio3d: an R package for the comparative analysis of protein structures. *Bioinformatics*, **22**, 2695–2696.

Hamelin,R. *et al.* (1994) TP53 gene mutations and p53 protein immunoreactivity in malignant and premalignant Barrett's esophagus. *Gastroenterology*, **107**, 1012–1018.

Hansson,J.H. *et al.* (1995) A de novo missense mutation of the beta subunit of the epithelial sodium channel causes hypertension and Liddle syndrome, identifying a proline-rich segment critical for regulation of channel activity. *Proc. Natl. Acad. Sci. USA*, **92**, 11495–11499.

Hollingsworth,S.A. *et al.* (2009) On the occurrence of linear groups in proteins. *Protein Sci.*, **18**, 1321–1325.

Hu,K.Q. and Settleman,J. (1997) Tandem SH2 binding sites mediate the RasGAP–RhoGAP interaction: a conformational mechanism for SH3 domain regulation. *EMBO J.*, **16**, 473–483.

Kaneko,T. *et al.* (2008) The SH3 domain—a family of versatile peptide-and protein-recognition module. *Front. Biosci.*, **13**, 4938–4952.

Kay,B.K. *et al.* (2000) The importance of being proline: the interaction of proline-rich motifs in signaling proteins with their cognate domains. *Faseb J.*, **14**, 231–241.

Khrunin,A. *et al.* (2010) Genetic polymorphisms and the efficacy and toxicity of cisplatin-based chemotherapy in ovarian cancer patients. *Pharmacogenomics J.*, **10**, 54.

Koshland,D.E.Jr (1995) The key–lock theory and the induced fit theory. *Angew. Chem. Int. Ed. Engl.*, **33**, 2375–2378.

Kuriyan,J. and Cowburn,D. (1997) Modular peptide recognition domains in eukaryotic signaling. *Annu. Rev. Biophys. Biomol. Struct.*, **26**, 259–288.

Leusen,J. *et al.* (1994) 156Pro–> Gln substitution in the light chain of cytochrome b558 of the human NADPH oxidase (p22-phox) leads to defective translocation of the cytosolic proteins p47-phox and p67-phox. *J. Exp. Med.*, **180**, 2329–2334.

Li,S.S.-C. (2005) Specificity and versatility of SH3 and other proline-recognition domains: structural basis and implications for cellular signal transduction. *Biochem. J.*, **390**, 641–653.

Luo,L. *et al.* (2016) The binding of syndapin SH3 domain to dynamin proline-rich domain involves short and long distance elements. *J. Biol. Chem.*, **291**, 703108.

Ma,K. *et al.* (2001) Polyproline II helix is a key structural motif of the elastic PEVK segment of titin. *Biochemistry*, **40**, 3427–3438.

Mansiaux,Y. *et al.* (2011) Assignment of PolyProline II conformation and analysis of sequence–structure relationship. *PLoS One*, **6**, e18401.

Martin,C. *et al.* (2014) Silaproline helical mimetics selectively form an all-trans PPII helix. *Chemistry A Eur. J.*, **20**, 14240–14244.

Mayer,B.J. (2001) SH3 domains: complexity in moderation. *J. Cell Sci.*, **114**, 1253–1263.

Mayer,B.J. and Eck,M.J. (1995) SH3 domains: minding your p's and q's. *Curr. Biol.*, **5**, 364–367.

Narwani,T.J. *et al.* (2017) Recent advances on polyproline II. *Amino Acids*, **49**, 705–713.

Nguyen,J.T. *et al.* (2000) Improving SH3 domain ligand selectivity using a non-natural scaffold. *Chem. Biol.*, 7, 463–473.

Obuchowski,P.L. and Jacobs-Wagner,C. (2008) PflI, a protein involved in flagellar positioning in *Caulobacter crescentus*. *J. Bacteriol.*, **190**, 1718–1729.

Pawson,T. and Scott,J.D. (1997) Signaling through scaffold, anchoring, and adaptor proteins. *Science*, **278**, 2075–2080.

Saksela,K. and Permi,P. (2012) SH3 domain ligand binding: What's the consensus and where's the specificity?. *FEBS Lett*, **586**, 2609–2614.

Ravi Chandra,B. *et al.* (2004) Distribution of proline-rich (PxxP) motifs in distinct proteomes: functional and therapeutic implications for malaria and tuberculosis. *Protein. Eng. Des. Sel.*, **17**, 175–182.

Stapley,B.J. and Creamer,T.P. (1999) A survey of left-handed polyproline II helices. *Protein Sci.*, **8**, 587–595.

Teyra,J. *et al.* (2017) Comprehensive analysis of the human SH3 domain family reveals a wide variety of non-canonical specificities. *Structure.*, **25**, 1598–1610.e1593.

Tossavainen,H. *et al.* (2016) Structural basis of the high-affinity interaction between the alphavirus nonstructural protein-3 (nsP3) and the SH3 domain of amphiphysin-2. *J Biol Chem.*, **291**, 16307–17.

Valenzuela-Iglesias,A. *et al.* (2015) Profilin1 regulates invadopodium maturation in human breast cancer cells. *Eur. J. Cell Biol.*, **94**, 78–89.

Wagih,O. (2017) ggseqlogo: a versatile R package for drawing sequence logos. *Bioinformatics*, **33**, 3645–3647.

Zarrinpar,A. *et al.* (2003) The structure and function of proline recognition domains. *Sci. STKE*, **2003**, RE8.